

Search for New Physics with Photons and Exclusive Z Production at the Tevatron

Dan Krop¹ on behalf of the CDF and DØ Collaborations

¹Enrico Fermi Institute, University of Chicago, Chicago, Illinois 60637

DOI: will be assigned

We report the results of searches for non-standard model phenomena in photon final states and a search for exclusive Z boson production. These searches use data from $p\bar{p}$ collisions at $\sqrt{s} = 1.96$ TeV collected with the CDF and DØ detectors at the Fermilab Tevatron corresponding to $1.0 - 4.2 \text{ fb}^{-1}$ of integrated luminosity. No disagreement of data with standard model predictions is observed. We report limits on the parameters of several models including anomalous triple gauge couplings, large extra dimensions, fermiophobic Higgs models, and supersymmetry.

1 Introduction

The standard model (SM) of particle physics [1] has been remarkably successful at predicting the details of almost all observed high energy physics processes. However, because the predicted high energy behavior of the SM becomes unphysical at an interaction energy of a few TeV we know that new physical phenomena are required. In this document we present the results of searches for phenomena that are beyond the standard model (BSM) using final states containing photons. The data used for these searches are obtained with the CDF and DØ detectors at the Fermilab Tevatron, where protons collide with antiprotons at $\sqrt{s} = 1.96$ TeV. Additionally, we present a search for exclusive Z production where the p and \bar{p} emerge from the collision intact. The CDF and DØ detectors are described in detail in Refs. [2] and [3], respectively.

2 Exclusive Z production

The CDF collaboration has performed a search for the exclusive production of Z bosons decaying to a $\mu^+\mu^-$ or e^+e^- pair and a measurement of the cross section for exclusive $\mu^+\mu^-$ and e^+e^- production with dilepton invariant mass $M_{ll} > 40$ GeV and $|\eta_l| < 4$ ¹. The analysis requires two

¹We use a cylindrical coordinate system in which ϕ is the azimuthal angle, r is the radius from the nominal beam line, and z points in the proton beam direction. The transverse ($r - \phi$) plane is perpendicular to the z axis. Transverse momentum and energy are the respective projections of momentum measured in the tracking system and energy measured in the calorimeter system onto the $r - \phi$ plane, and are defined as $p_T = p \sin \theta$ and $E_T = E \sin \theta$. Here, θ is the polar angle measured with respect to the interaction vertex. Missing E_T ($\vec{\cancel{E}}_T$) is defined by $\vec{\cancel{E}}_T = -\sum_i E_T^i \hat{n}_i$, where i is the calorimeter tower number for $|\eta| < 3.6$, and \hat{n}_i is a unit vector perpendicular to the beam axis and pointing at the i^{th} tower. The pseudorapidity η is defined as $-\ln(\tan(\theta/2))$, where θ is measured with respect to the origin of the detector. We define the magnitude $E_T = |\vec{\cancel{E}}_T|$. We use the convention that “momentum” refers to pc and “mass” to mc^2 .

oppositely-charged leptons of the same flavor with $M_{ll} > 40$ GeV and $p_T^l > 20$ GeV. For the exclusive Z search, a subsample is selected with $82 < M_{ll} < 98$ GeV and $p_T^l > 25$ GeV. Events containing additional tracks or energy deposition in any calorimeter above that expected from noise are rejected. Events are also rejected if any beam shower counter (BSC) has hits above threshold². The acceptance for reconstructing exclusive dilepton events is calculated using the LPAIR [6] Monte Carlo (MC) event generator while the corresponding acceptance for exclusive Z production is obtained from PYTHIA [7]. The detector response to these events is simulated with GEANT [8]. No events pass the exclusive $Z \rightarrow l^+l^-$ selection criteria and we therefore set an upper limit on the cross section of exclusive Z production at the Tevatron of $\sigma_{excl}(Z) < 0.96$ pb at 95% confidence level (C.L.). Eight exclusive dilepton events are observed with an estimated background of 1.45 ± 0.61 events. Figure 1 shows the dilepton invariant mass distribution of these events as well as the LPAIR prediction. The cross section for exclusive dilepton production in the region $M_{ll} > 40$ GeV is found to be $\sigma_{obs} = 0.24_{-0.10}^{+0.13}$ pb, which is in good agreement with the LPAIR prediction of 0.256 pb.

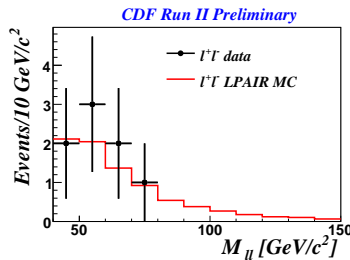


Figure 1: The CDF exclusive Z production search: the dilepton invariant mass distribution observed and the LPAIR prediction with the GEANT simulation scaled to account for acceptance and luminosity.

3 Searches in the $\gamma \cancel{E}_T$ final state

The $\gamma \cancel{E}_T$ channel is useful both as a test of SM parameters, through the $Z\gamma \rightarrow \nu\bar{\nu}\gamma$ process, and to search for BSM processes that contain a photon where the missing energy is associated with some new, undetected particle.

The DØ collaboration performs a measurement of the $Z\gamma \rightarrow \nu\bar{\nu}\gamma$ cross section and searches for anomalous triple gauge couplings [9] using 3.6 fb^{-1} of data. It also searches [10] for pairs of close-by leptons in the $\gamma \cancel{E}_T$ final state and sets limits on SUSY models containing “dark” sectors inspired by possible dark matter signals in cosmic ray detection experiments [11] using 4.1 fb^{-1} of data. Finally, both DØ [12] and CDF [13] search for large extra dimensions (LED) [14] that would leave a $\gamma \cancel{E}_T$ signature in the detector through the emission of an undetected Kaluza-Klein graviton (G_{KK}), $q\bar{q} \rightarrow \gamma G_{KK}$.

²The BSC consists of scintillation counters located along the beam pipe at high pseudorapidities, $3.6 < |\eta| < 7.4$.

3.1 Triple gauge coupling

The SM has no tree-level $Z\gamma\gamma$ or $ZZ\gamma$ couplings, leading to a small cross section for $Z\gamma$ production. The presence of such couplings in BSM theories can enhance the yield, especially at higher values of photon E_T . Anomalous couplings can be parametrized using a set of eight complex parameters h_i^V ($i = 1, \dots, 4; V = Z, \gamma$) of the form $h_i^V = h_{i0}/(1 + \hat{s}/\Lambda^2)^n$ [15]. The DØ collaboration sets limits on the real part of the anomalous coupling, $Re(h_{i0}^V)$, referred to as ATGC in the following.

The analysis requires one photon candidate with $E_T > 90$ GeV and $|\eta| < 1.1$ and missing transverse energy of $\cancel{E}_T > 70$ GeV. Events containing jets with $E_T > 15$ GeV, any muon, and additional electromagnetic objects with $E_T > 15$ GeV are rejected. Furthermore, to suppress non-collision backgrounds, a pointing algorithm [16] is used to reconstruct the photon trajectory. The z position of the interaction vertex predicted by the pointing algorithm must be within 10 cm of the chosen reconstructed primary vertex. 51 events are observed with a background prediction, excluding $Z\gamma \rightarrow \nu\bar{\nu}\gamma$, of $17.3 \pm 0.6(\text{stat.}) \pm 2.3(\text{syst.})$. The cross section of $Z\gamma$ production multiplied by the branching fraction of the Z into neutrinos is thus measured to be 32 ± 9.2 fb with a significance of 5.1σ . This agrees well with the SM prediction of 39 ± 4 fb.

To test for the presence of a BSM signal, the observed photon E_T spectrum is compared with that expected from the SM. Figure 2 shows this spectrum. No excess over background predictions is observed. Using this distribution and Poisson statistics, limits of $|h_{30}^\gamma| < 0.033$, $|h_{40}^\gamma| < 0.0017$, $|h_{30}^Z| < 0.033$, and $|h_{40}^Z| < 0.0017$ are set at 95% C.L.

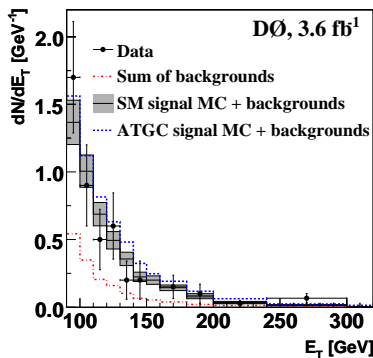


Figure 2: The DØ $\gamma\cancel{E}_T$ triple gauge coupling search: Photon E_T spectrum in data (solid circles), the sum of MC signal and backgrounds (dash-dot line), and for the ATGC prediction with $h_{30}^\gamma = 0.09$ and $h_{40}^\gamma = 0.005$ (dashed line). The shaded band corresponds to the ± 1 s.d. total uncertainty on the predicted sum of the SM signal and background.

3.2 Dark photons

The DØ dark photon analysis searches for events with a photon, large \cancel{E}_T , and two close-by leptons as indicated by the example diagram on the left side of Fig. 3. The $\gamma\cancel{E}_T$ base sample is selected by requiring a photon with $E_T > 30$ GeV and $\cancel{E}_T > 20$ GeV. Dark photon candidates are formed by selecting pairs of oppositely charged tracks that are close-by spatially, $\Delta R < 0.2$, and originate from the same point along the beamline, $|\Delta z| < 2$ cm. The QCD

background is suppressed by requiring that no track has its azimuthal angle aligned with the photon, $0.4 < \Delta\phi_{\gamma, track} < 2.74$. For electron pair candidates, the calorimeter depositions are expected to overlap, so the dark photon candidate is required to match an electromagnetic cluster with $E_T > 10$ GeV, $EM_{frac} > 97\%$, and $\mathcal{I} < 0.1^3$. No evidence for a peak in the dilepton mass spectrum is observed. A modified version of the SUSYHT [17] generator is used along with PYTHIA [7] and GEANT [8] to generate the signal hypotheses in the dilepton mass spectrum. Limits are then set from the dilepton mass spectrum using a log-likelihood ratio (LLR) statistic method [18]. These limits are interpreted in terms of the branching fraction of the neutralino into the dark photon, $\mathcal{B} = Br(\tilde{\chi}_1^0 \rightarrow \gamma_D \tilde{X})$. The right side of Fig. 3 shows the chargino mass limit as a function of \mathcal{B} for three representative dark photon masses. For dark photon masses of 0.2, 0.782, and 1.5 GeV chargino masses of 230, 142, and 200 GeV are excluded at the 95% C.L., respectively.

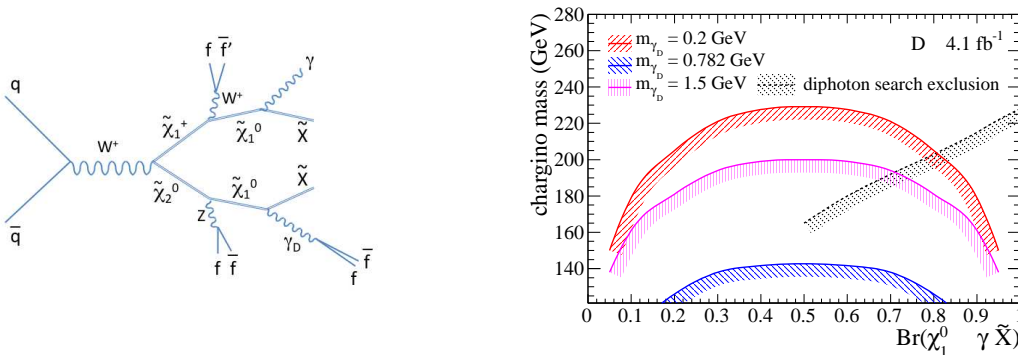


Figure 3: The DØ dark photon search. On the left: One of the diagrams giving rise to a photon, dark photon (γ_D), and large \cancel{E}_T due to escaping darkinos (\tilde{X}). On the right: The dependence of the excluded chargino masses on the branching ratio of the neutralino into a photon are given for dark photon masses of 0.2, 0.782, and 1.5 GeV. The black contour corresponds to the exclusion from a previous diphoton search [19].

3.3 Large extra dimensions

The CDF and DØ $\gamma\cancel{E}_T$ LED searches use data corresponding to 2.0 fb^{-1} and 2.7 fb^{-1} of $p\bar{p}$ collisions, respectively. The analyses require one central photon with $E_T > 90$ GeV and $\cancel{E}_T > 50(70)$ GeV for CDF(DØ). Events with additional high p_T tracks or jets are removed. The DØ analysis uses the photon pointing technique mentioned above to reduce non-collision backgrounds. The CDF analysis requires the photon to be in time with the $p\bar{p}$ collision and uses topological variables to reduce these backgrounds. Neither analysis observes a significant excess in the data over the expected SM contribution. CDF observes 40 events with an expected background of 46.3 ± 3.0 events and DØ observes 51 versus an expected background of 49.9 ± 4.1 . CDF reports lower limits on the fundamental Planck scale, M_D , of 1080–900 GeV for $n_d = 2-6$

³The electromagnetic fraction, EM_{frac} , is defined as the fraction of total energy of the cluster deposited in the EM section of the calorimeter. The calorimeter isolation, \mathcal{I} , is defined as $\mathcal{I} = [E_{tot}(0.4) - E_{EM}(0.2)] / E_{EM}(0.2)$. The 0.2 and 0.4 refer to radius of the cone in ΔR which is used to calculate the energy of the cluster.

at 95% C.L while DØ obtains limits of 970–804 GeV for $n_d = 2-8$, where n_d refers to the number of extra dimensions.

4 Searches in the $\gamma\gamma$ final state

The diphoton channel is used by DØ in an LED search [20] and by both CDF [21] and DØ [22] in fermiophobic Higgs searches. DØ uses data corresponding to 1.1 fb^{-1} of $p\bar{p}$ collisions for the LED search and 4.2 fb^{-1} for the fermiophobic Higgs search. CDF uses data corresponding to 3.0 fb^{-1} of collisions for its fermiophobic Higgs search.

4.1 Large extra dimensions

The DØ diphoton LED search selection requires two EM objects, each having $E_T > 25 \text{ GeV}$ and being both in the central EM calorimeter ($|\eta| < 1.1$) or one in the central and one in the forward EM calorimeter ($1.5 < |\eta| < 2.4$). Because no track selection is made, the analysis combines the dielectron and diphoton channels. The normalization of the QCD background is obtained by fitting M_{diEM} in the range of 60 – 140 GeV, where no LED signal is expected, to a combination of SM $ee/\gamma\gamma$ and QCD shapes, with the QCD shape being obtained from a dataset where an EM object fails shower profile requirements. No discrepancy from the backgrounds prediction is observed and lower limits on M_S^4 at the 95% C.L. are set: 1.62 TeV using the GRW [23] formalism and 2.09 – 1.29 TeV using the HLZ [24] formalism for $n_d = 2 - 7$.

4.2 Fermiophobic Higgs

The SM branching fraction for a low mass Higgs boson in the diphoton final state, $Br(h \rightarrow \gamma\gamma)$, has a maximal value of approximately 0.2% for Higgs boson masses of about 120 GeV. In so-called “fermiophobic” Higgs models, $Br(h \rightarrow \gamma\gamma)$ is enhanced [25]. CDF selects photons having $E_T > 15 \text{ GeV}$ and requires them to be either both central ($|\eta| < 1.05$) or one to be central and one forward ($1.2 < |\eta| < 2.8$). DØ selects two central ($|\eta| < 1.1$) photons with $E_T > 20 \text{ GeV}$. CDF requires $p_T(\gamma\gamma) > 75 \text{ GeV}$ and DØ selects $p_T(\gamma\gamma) > 35 \text{ GeV}$. The DØ analysis uses an artificial neural network (ANN) [26] to reduce the contribution from jets misidentified as photons and a matrix background subtraction method [27] to obtain detailed estimates of γ +jet and di-jet backgrounds. After no excess is observed in the diphoton mass distribution, this distribution is used to set limits on fermiophobic Higgs models using a modified frequentist approach [18, 28]. CDF also observes no excess in the diphoton mass spectrum and approximates the background via a fit to a smooth curve; limits are set using a binned-likelihood method and Poisson fluctuation of the $M_{\gamma\gamma}$ bin contents. Figure 4 shows $M_{\gamma\gamma}$ distributions from both analyses. DØ(CDF) obtains a limit of $M(h_f) > 102.5(106) \text{ GeV}$ at 95% C.L.

5 Searches for supersymmetry in the $\gamma\gamma \cancel{E}_T$ final state

The CDF and DØ collaborations have searched for gauge-mediated supersymmetry breaking (GMSB) [29] in 2.6 and 1.1 fb^{-1} of $p\bar{p}$ collisions, respectively. In GMSB, the next-to-lightest supersymmetric particle $\tilde{\chi}_1^0$ may decay to a gravitino via $\tilde{\chi}_1^0 \rightarrow \tilde{G}\gamma$. Pair production of massive

⁴ M_S is the ultraviolet cutoff of the sum over Kaluza-Klein states, also called the “effective Planck scale”

SUSY particles would result in a final state with two photons and large \cancel{E}_T due to the undetected gravitino. Both analyses consider the minimal Snowmass Slope SPS 8 [30] GMSB model to quote results as a function of $\tilde{\chi}_1^0$ mass and lifetime. DØ(CDF) requires two central photons with $E_T > 25(13)$ GeV. To reduce the bias of the \cancel{E}_T measurement arising from mismeasurement of the jet transverse momentum, DØ requires the highest E_T jet to be separated from the \cancel{E}_T by no more than 2.5 radians. CDF requires $\Delta\phi(\gamma_1, \gamma_2) < \pi - 0.15$, $H_T^5 > 200$ GeV, and \cancel{E}_T significance⁶ > 3 . DØ uses the photon pointing algorithm to suppress non-collision backgrounds while CDF achieves this suppression by requiring the photon candidates to be in time with the $p\bar{p}$ collision and by using topological variables. After all selections, DØ observes 3 events with $\cancel{E}_T > 60$ GeV with a background expectation of 1.6 ± 0.4 events. CDF observes no events with a background expectation of 1.23 ± 0.38 . 95% C.L. limits of $m(\tilde{\chi}_1^0) > 125$ GeV and $m(\tilde{\chi}_1^0) > 149$ GeV are obtained from DØ and CDF for $\tau(\tilde{\chi}_1^0) = 0$, respectively.

6 Signature-based searches with photons

Motivated by the unknown nature of possible BSM signals in the Tevatron dataset, the CDF collaboration presents search analyses which test whether a particular signature is consistent with SM predictions and do not set limits on specific exotic models. Two of these so-called “signature-based” searches are presented: an analysis of the $l\gamma b\cancel{E}_T$ final state [33] and an analysis of the $\gamma bj\cancel{E}_T$ final state [34].

6.1 The $l\gamma b\cancel{E}_T$ final state

The $l\gamma b\cancel{E}_T$ analysis requires events with a central γ candidate having $E_T > 10$ GeV, a central electron or muon with $E_T > 20$ GeV, $\cancel{E}_T > 20$ GeV, and a b -tagged⁷ jet with $E_T > 15$ GeV. Events passing these requirements form a “base” sample. A second search is constructed to enhance the contribution of $t\bar{t}\gamma$ events by additionally requiring $H_T > 200$ GeV and $N(\text{jets}) > 3$. 28 events are observed in the base sample with a corresponding SM background prediction of $31.0_{-3.9}^{+4.1}$ events. In the enhanced sample, 16 events are observed with a background prediction of $11.2_{-2.1}^{+2.3}$ events. The probability that non- $t\bar{t}\gamma$ backgrounds produce 16 or more events is calculated to be 1%. Assuming this excess to be due to SM $t\bar{t}\gamma$ production, the $t\bar{t}\gamma$ cross section is calculated to be $\sigma_{t\bar{t}\gamma} = 0.15 \pm 0.08$ pb.

6.2 The $\gamma bj\cancel{E}_T$ final state

The event selections for the $\gamma bj\cancel{E}_T$ analysis are as follows: one central photon with $E_T > 25$ GeV, two jets with $|\eta| < 2.0$ and E_T at least one of which must be b -tagged, $\cancel{E}_T > 25$ GeV, $\Delta R > 0.4$ for any two objects in the event, and $\Delta\phi(\cancel{E}_T, \text{jet})_i > 0.3$ for any jet. The CDF collaboration observes 617 events while the SM prediction is $607 \pm 74(\text{stat.}) \pm 86(\text{syst.})$; no deviation from the SM prediction is observed. The consistency of the distributions of 11 kinematic variables with the SM prediction is tested by using the Kolmogorov-Smirnoff (KS) test; the probability that the SM hypothesis is consistent with the observed distributions range from 7 – 99%, again

⁵ H_T is defined as the scalar sum p_T of all identified objects in the event

⁶ \cancel{E}_T significance is defined as $-\log(\mathcal{P})$, where \mathcal{P} is the probability form \cancel{E}_T drawn from the expected mismeasured \cancel{E}_T distribution to be equal to or larger than the observed \cancel{E}_T

⁷ A b -tagging algorithm identifies jets containing b hadrons through the presence of a b -hadron decay vertex displaced from the beam line [35].

indicating agreement with the SM hypothesis. Finally, 11 additional selections are applied to enhance any possible signals on the tails of kinematic distribution. No deviation from the SM hypothesis is observed in any of these additional selections.

7 Conclusions

The CDF and DØ collaborations have a far-reaching program to search for new physics in photon final states. No significant deviation from the SM has yet been observed in data corresponding to between $1 - 4.2 \text{ fb}^{-1}$ of $p\bar{p}$ collisions. However, none of the results presented in this document utilize more than half of the expected full dataset from the Tevatron by the end of Run II. As more data is collected, we expect to see many interesting results from both experiments.

Acknowledgements

The author acknowledges and thanks the CDF exotic and DØ new phenomena group conveners for their helpful suggestions to improve the presentation of these results and Yuri Gershtein for his helpful explanation of the dark photon result.

References

- [1] S.L. Glashow, Nucl. Phys. **22**, 588 (1961); S. Weinberg, Phys. Rev. Lett. **19**, 1264 (1967);
- [2] D. E. Acosta *et al.* [CDF Collaboration], Phys. Rev. D **71**, 052003 (2005).
- [3] V. M. Abazov *et al.* [D0 Collaboration], Nucl. Instrum. Meth. A **565**, 463 (2006).
- [4] T. Aaltonen *et al.* [CDF Collaboration], Phys. Rev. Lett. **102**, 222002 (2009).
- [5] L. Motyka and G. Watt, Phys. Rev. D **78**, 014023 (2008).
- [6] J. A. M. Vermaseren, Nucl. Phys. B **229**, 347 (1983); S. P. Baranov, O. Duenger, H. Shooshtari, and J. A. M. Vermaseren, In **Hamburg 1991, Proceedings, Physics at HERA, vol. 3* 1478-1482 (see HIGH ENERGY PHYSICS INDEX 30 (1992) No. 12988)*.
- [7] T. Sjostrand *et al.*, Comput. Phys. Commun. **135**, 238 (2001).
- [8] R. Brun and F. Carminati, CERN Program Library Long Writeup, W5013 (1993) [unpublished].
- [9] V. M. Abazov *et al.* [D0 Collaboration], Phys. Rev. Lett. **102**, 201802 (2009).
- [10] V. M. Abazov *et al.* [D0 Collaboration], FERMILAB-PUB-09-229-E, arXiv:0905.1478v2 [hep-ex], (2009).
- [11] N. Arkani-Hamed, D. P. Finkbeiner, T. R. Slatyer and N. Weiner, Phys. Rev. D **79**, 015014 (2009); N. Arkani-Hamed and N. Weiner, JHEP **0812**, 104 (2008);
- [12] E. Carrera [D0 Collaboration], arXiv:0180.1331 [hep-ex].
- [13] T. Aaltonen *et al.* [CDF Collaboration], Phys. Rev. Lett. **101**, 181602 (2008).
- [14] N. Arkani-Hamed, S. Dimopoulos, and G. R. Dvali, Phys. Lett. B **429**, 263 (1998).
- [15] U. Baur and E. Berger, Phys. Rev. D **47**, 4889 (1993).
- [16] S. Keisisoglou, Brown University, Ph.D. Thesis, FERMILAB-THESIS-2004-44, UMI-31-74625 (2004).
- [17] A. Djouadi, M. M. Muehlleitner, M. Spira, Acta Phys. Pol. B **38**, 635 (2007).
- [18] T. Junk, Nucl. Instrum. Methods A **434**, 435 (1999); A. Read, CERN 2000-005 (200).
- [19] V. M. Abazov *et al.* [D0 Collaboration], Phys. Lett. B **659**, 856 (2008).
- [20] V. M. Abazov *et al.* [D0 Collaboration], Phys. Rev. Lett. **102**, 051501 (2009).

- [21] T. Aaltonen *et al.* [CDF Collaboration], FERMILAB-PUB-09-218-E, arXiv:0905.0413 [hep-ex] (2009).
- [22] V. M. Abazov *et al.* [D0 Collaboration], D0 Note 5880-CONF (2009).
- [23] G. Giudice, R. Rattazzi, and J. Wells Nucl. Phys. B **544**, 3 (1999).
- [24] T. Han, J. Lykken, and R. Zhang, Phys. Rev. D **59** 105006 (1999).
- [25] S. Mrenna and J. D. Wells, Phys. Rev. D **63**, 015006 (2001).
- [26] C. Peterson, T. Rognvaldsson, and L. Lonnblad, Lund University Preprint LU-TP 93-29.
- [27] Y. Liu, Ph.D Thesis, FERMILAB-THESIS-2004-37 (2004).
- [28] W. Fisher, FERMILAB-TM-2836-E (2007).
- [29] S. Ambrosiano, G. L. Kane, G. D. Kribs, S. P. Martin, and S. Mrenna, Phys. Rev. D **54**, 5395 (1996); C. H. Chen and J. F. Gunion, Phys. Rev. D **58**, 075005 (1998).
- [30] B. C. Allanach *et al.*, Eur. Phys. J. C **25**, 113 (2002).
- [31] V. M. Abazov *et al.* [D0 Collaboration], Phys. Lett. B **659**, 856 (2008)
- [32] T. Aaltonen *et al.* [CDF Collaboration], CDF Note 9625 (2008).
- [33] T. Aaltonen *et al.* [CDF Collaboration], FERMILAB-PUB-09-280-E, arXiv:0906.0518 [hep-ex] (2009).
- [34] T. Aaltonen *et al.* [CDF Collaboration], FERMILAB-PUB-09-221-E, arXiv:0905.0231 [hep-ex] (2009).
- [35] D. Acosta *et al.* [CDF Collaboration] Phys. Rev. D **71**, 052003 (2005); C. Neu, FERMILAB-CONF-06-162-E (2006).

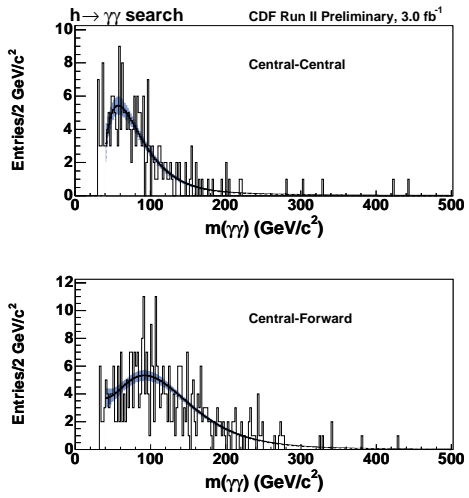
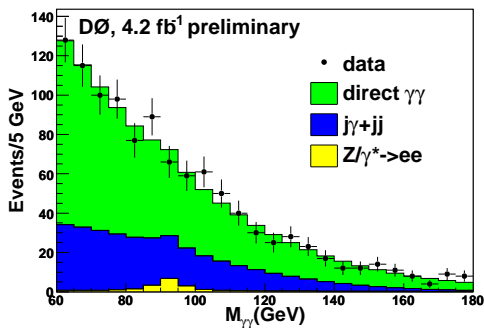


Figure 4: Fermiophobic Higgs searches: Invariant mass distributions of diphoton candidates for the $D\bar{O}$ search on the left and the CDF search on the right. CDF plots the central-central and central-forward diphoton candidates separately and has the results of fits to a smooth curve overlaid on the distributions.